Università di Pisa

Dottorato di Ricerca in
Tecnologie per la Salute: Valutazione e Gestione delle Innovazioni nel Settore Biomedicale

Prostate cancer: pre-treatemnt evaluation with Magnetic Resonance Imaging and three-dimensional 1H-Magnetic Resonance Spectroscopy

Presidente:
Prof. Andrea Pietrabissa

Tutor:

Prof. Davide Caramella

Candidato:

Dr.ssa Sabina Giusti

Anno Accademico 2006/2007

INDEX

RESEARCH PROJECT

Magnetic resonance imaging and hydrogen 1 MR spectroscopy of the prostate gland are performed during the same examination with a conventional clinical MR unit.

Prostate zonal anatomy and prostate cancer are best depicted on multiplanar T2-weighted MR images. MR imaging and 1H MR spectroscopy are not used as an initial diagnostic tool. Their use in tumor detection is reserved for patients with elevated prostate-specific antigen levels in whom previous biopsy results were negative. The use of MR imaging and 1H MR spectroscopy for the evaluation of tumor location, local extent (extracapsular extension and/or seminal vesicle invasion), volume, and aggressiveness is generating strong clinical interest.

In staging and treatment planning, MR imaging has been shown to have an incremental value additive to the value of clinical nomograms. Furthermore, anatomic and metabolic mapping of the prostate gland with 1H MR spectroscopy offers the possibility of optimizing treatment planning (watchful waiting, surgery, or radiation therapy [intensity-modulated radiation therapy or brachytherapy]), thus further expanding the role of MR imaging in the achievement of patient-specific, individualized treatment.

INTRODUCTION

Prostate cancer is the most frequent malignancy of the male genitourinary tract, with an incidence in Europe of approximately 30 per 100.000 [48,49]. MRI of the prostate with a combined pelvic and endorectal coil has become an accepted method for staging prostate cancer. The advantages of this technique get results especially in local staging sensitivity, with a better judgement of surrounding structures [50,51]. Three-dimensional 1H-spectroscopy (3D MRS) of the prostate with evaluation of the metabolites choline, creatine, and citrate is a promising method for detecting prostate carcinomas which in particular show a higher choline and a reduced citrate level in comparison with healthy prostatic tissue [52,53].

The first objective of our study was to assess sensitivity, specificity and accuracy of 3-D MRI and 3D MRS in patients with high prostate-specific antigen (PSA) levels and biopsy proven prostate carcinoma, candidate to radical prostatectomy.

The second purpose was to find a cut-off value of (Cho+Cr)/Cit ratio to discriminate between normal peripheral zone tissue and cancer.

Besides we find a correlation between (Cho+Cr)/Cit ratio and histologic Gleason score.

MATERIALS AND METHODS

Patient Characteristics

Our study included a total of 27 patients (median age, 65 years; age range, 48-77 years; median PSA, 10.37 ng/ml, PSA range, 4.2-39 ng/ml) who underwent endorectal MRI and 3D-MRS followed by radical prostatectomy between January 2005 and February 2007. Informed consent was obtained from all patients according to an institutionally approved research protocol. Patients with a histologically proven prostate carcinoma and without any contraindications for MRI examination of the prostate were included in our study. Patients with previous surgery, radiation therapy or under ongoing hormonal therapy were not included. A minimum delay of 4-6 weeks was required between biopsy and MRI and MRS to minimize biopsy artifacts.

The average time elapsed between the combined MR and MRS examination and radical prostatectomy was 15 days. Following surgery, radical prostatectomy specimens were submitted for wholemount step-section pathologic evaluation.

MR Image Acquisition Protocol

Imaging of the prostate was performed on a 1.5-T Siemens scanner (Magnetom Symphony Maestro; Siemens Medical Solutions, Erlangen, Germany) with a combined pelvic phased-array coil and endorectal coil (MRInnervu; Medrad, Indianola, USA). No contrast medium was used for imaging. The endorectal coil was inserted and inflated with approximately 60 ml air. No drugs was administered to reduce bowel motility.

The sequence protocol consisted of transversal (tra), coronal (cor) and sagittal (sag) T2-weighted fast spin echo (FSE) sequences. T1-weighted FSE sequence was used to detect the presence of post-biopsy haemorrhage and for assessing lymph node status of the pelvis.

Sequence data

– T2w FSE tra: turbo factor 23, TR 4300 ms, TE 117 ms, slice thickness 3.0 mm, FoV 160 mm, Gap 0.8 mm, matrix 230x256, NEX 2, scan time 4’32’’

– T2w FSE sag: turbo factor 25, TR 3500 ms, TE 107 ms, slice thickness 3.0 mm, FoV 200 mm, Gap 0.8 mm, matrix 224x320, NEX 2, scan time 3’55’’

– T2w FSE cor: turbo factor 25, TR 3500 ms, TE 107 ms, slice thickness 3.0 mm, FoV 180 mm, Gap 0.8 mm, matrix 256x256, NEX 2, scan time 4’25’’

– T1w FSE tra: turbo factor 3, TR 500-600 ms, TE 15 ms, slice thickness 3.0 mm, FoV 160 mm, Gap 0.8 mm, matrix 196x256, NEX 2, scan time 4’19’’

Three-dimensional 1H-spectroscopy (3D MRS)

MRS data were acquired by a three-dimensional chemical shift imaging (3D CSI) double spin-echo point-resolved spatially localized spectroscopic (PRESS) sequence [54] on a Magnetom Symphony Maestro 1.5-T scanner (Siemens Medical Solutions). The body coil was used for homogenous excitation, and an endorectal coil for signal reception, granting maximum signal-to-noise ratio (SNR). TE = 120 ms allowed in-phase detection of the citrate signal. We resorted to k-space weighted acquisition to make optimal use of the scan time: For TR = 1.300 ms and four averages, the scan time was 11 min 12 s.

Along the spatial dimensions a Hamming filter was applied. The voxel size was 6.7×6.7×6.7 mm^3. The field map-based automatic shimming procedure of the system was applied. The VoI was positioned closely around the prostate, and a reference frequency corresponding to 2.9 ppm (i.e., the centre of the citrate and choline resonances of interest) was used. Additionally, simultaneous spectral suppression of the water and the lipid signals was performed and up to eight spatially selective saturation bands were interactively positioned. We obtained integral values by fitting Gaussian lineshape functions to the resulting absorption spectra. For further analysis, integral ratios were used (Cho+Cr)/Cit. The spectral grid was superimposed on the reference images in transversal, coronal and sagittal orientations. The spectra were automatically post-processed and reconstructed with commercially available software.

In patients with histologically proven prostate carcinoma we indicated the voxels covering tumorous lesions as “malignant voxels”; voxels covering non suspicious prostate tissue were defined as “normal voxels”.

Histopathologic analysis

Prostatectomy specimen whole-mount preparation consisted of its fixation in 10% formalin for 36 hours. The distal 5-mm portion of the apex was amputated and coned. The remainder of the gland was serially sliced from the apex to the base at 3–4 mm intervals, and slices were submitted for paraffin embedding as whole mounts. The seminal vesicles were amputated and submitted separately. After paraffin embedding, micro-slices were placed on glass slides and stained with haematoxylin and eosin. At pathologic analysis, a Gleason score was assigned to the whole cancer in the specimen according to the current clinical protocol at our institution. Besides, cancer foci were outlined by the pathologist with ink on whole-mount, apical, and seminal vesicle slices so to result grossly visible, and then photographed. These histological findings constituted our tumour maps.

Data analysis

All T2wi, T1wi and spectroscopic data sets were prospectively evaluated by two radiologists with different levels of experience in

evaluating prostate MR images and without prior knowledge of the PSA level or biopsy results.

Subsequently, after radical prostatectomy followed by histopathologic analysis, MR images and spectra previously obtained were compared with the results of pathologist by the same two radiologists in consensus. This correlation was performed just evaluating the whole right and the whole left lobe of the prostate. Lesions resulted malignant at histopathology and located within the apex or middle gland or in prostatic base were considered as involving the entire lobe. The same criteria was applied during the MR and MRS interpretation. This was to avoid erroneous samples obtained during trans-rectal US biopsy and leading to incorrect results.

At least, we merged the T2w MR images with the whole-mount sections. We used as landmarks the morphology of the gland and its normal anatomy, with particular regards to the apex, the base and the urethra. Thank to this accurately fusion we could consider as surely malignant those voxels completely enclosed within the tumorous zone outlined in ink from pathologist and as negative ones all the others.

Statistical analysis

Sensitivity, specificity and accuracy of biopsy, MRI, MRS and MRI+MRS readings were correlated with pathology results (gold standard); our data were calculated using a stastical software.

We entered the data of different variables (biopsy, MRI, MRS, MRI+MRS) in columns of the spreadsheet of the software and we correlated them with the gold standard variable (histopathology). We calculated sensitivity and specificity, accuracy, PPV and NPV for all possible threshold values.

To evaluate the concordance between the different diagnostic methods and the histopathologic results, we compared true positive data of biopsy, MRI alone, MRS alone and combined MRI+MRS with the results of histopathology, using Cohen's test and we obtained a K value for each comparison.

Retrospectively and related to pathologic results, we used ROC curves to calculate a cut-off value of (Cho+Cr)/Cit ratio that allowed us to discriminate between cancer and normal prostatic tissue in the peripheral zone.

RESULTS

26 of 27 patients who underwent MRI and MRS followed by radical prostatectomy, were included in the final analysis of spectroscopy data. Step section histopathology demonstrated stage pT2 disease in 18 patients, pT3 in 4 patients (unilateral extracapsular extension n=2, bilateral n=0, seminal vesicle extension n=0), pT4 in 4 patients.

In these 26 patients, a total of 43 locations of cancer were identified with step-section pathologic evaluation. Biopsy correctly detected 37 locations with 6 false-negative and 3 false-positive findings (sensitivity of 86%, specificity of 67%, accuracy of 83%, negative predictive value of 50%, and positive predictive value of 92%); MRI correctly detected 36 locations with 7 false-negative and 1 false-positive findings (sensitivity of 84%, specificity of 89%, accuracy of 85%, negative predictive value of 53%, and positive predictive value of 97%); MRS correctly detected 36 locations with 7 false-negative and 2 false-positive findings (sensitivity of 84%, specificity of 78%, accuracy of 83%, negative predictive value of 50%, and positive predictive value of 95%); MRI+MRS correctly detected 39 locations with 4 false-negative and 2 false-positive findings (sensitivity of 91%,

specificity of 78%, accuracy of 88%, negative predictive value of 64%, and positive predictive value of 95%).

Sensitivity, specificity, accuracy and positive and negative predictive values of biopsy, MRI, MRS and MRI+MRS for lobar localization of prostate cancer are listed in table 1 and histogram in figure 14 shows the gain in sensitivity, specificity, accuracy, PPV and NPV of MRI+MRS than biopsy .

	% Sensitivity	Specificity	%Accuracy	%P P V	%N P V
Biopsy	86	67	83	92	50
MRI	84	89	85	97	53
MRS	84	78	83	95	50
MRI+MRS	91	78	88	95	64

Table 1. Sensitivity, specificity, accuracy and positive and negative predictive values of biopsy, MRI, MRS and MRI+MRS for lobar localization of prostate cancer.

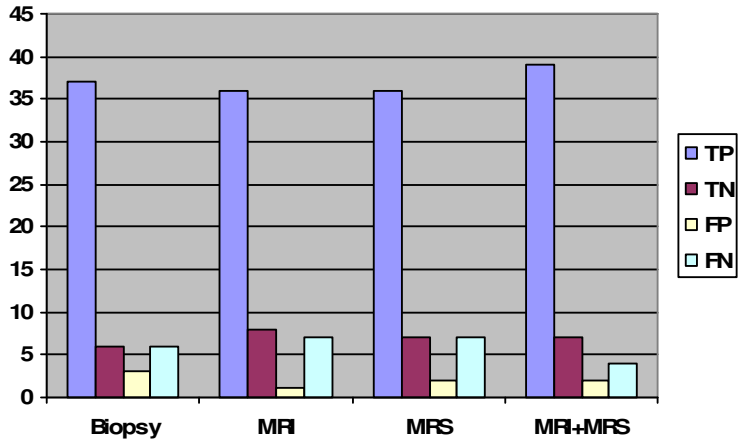

Fig.14.The histogram shows true positive (TP), true negative (TN), false positive (FP) and false negative (FN) value of the different methods compared with histology. Combined MRI and MRS shows a gain in TP and reduction on FP and FN compared with biopsy.

Using Cohen's test we compared the true positive values of the different diagnostic thecniques (biopsy, MRI and MRS alone and MRI+MRS) with the histopathologic results, to evaluate the degree of agreement between the differents diagnostic methods and the gold standard (histology). Cohen's test showed that biopsy had a lower degree of agreement with histology than MRI+MRS combined (0.559, moderate agreement versus 0.735, good agreement) [55] (table 2).

	K-value
Biopsy	0.559
MRI	0.581
MRS	0.563
MRI+MRS	0.735

Table 2. Cohen's test

Retrospectively basing on whole-mount sections and using a dedicated software we merged hystopathologic sections with the corresponding T2w images in order to obtain "neoplastic spectra" (n=37) from the malignant voxel exactly enclosed within the neoplastic area outlinked in ink from pathologist, and "control spectra" (n=66) from the voxels out of the signed neoplastic areas (fig 15).

. We obtained also related (Cho+Cr)/Cit ratios; the mean peak area ratio of (Cho+Cr)/Cit in tumorous lesions was 2,74 (± 4,6) and in control voxels 0.25 (± 0.16). The difference regarding the (Cho+Cr)/Cit ratio was highly significant between tumour and control voxels ($p<0.001$).

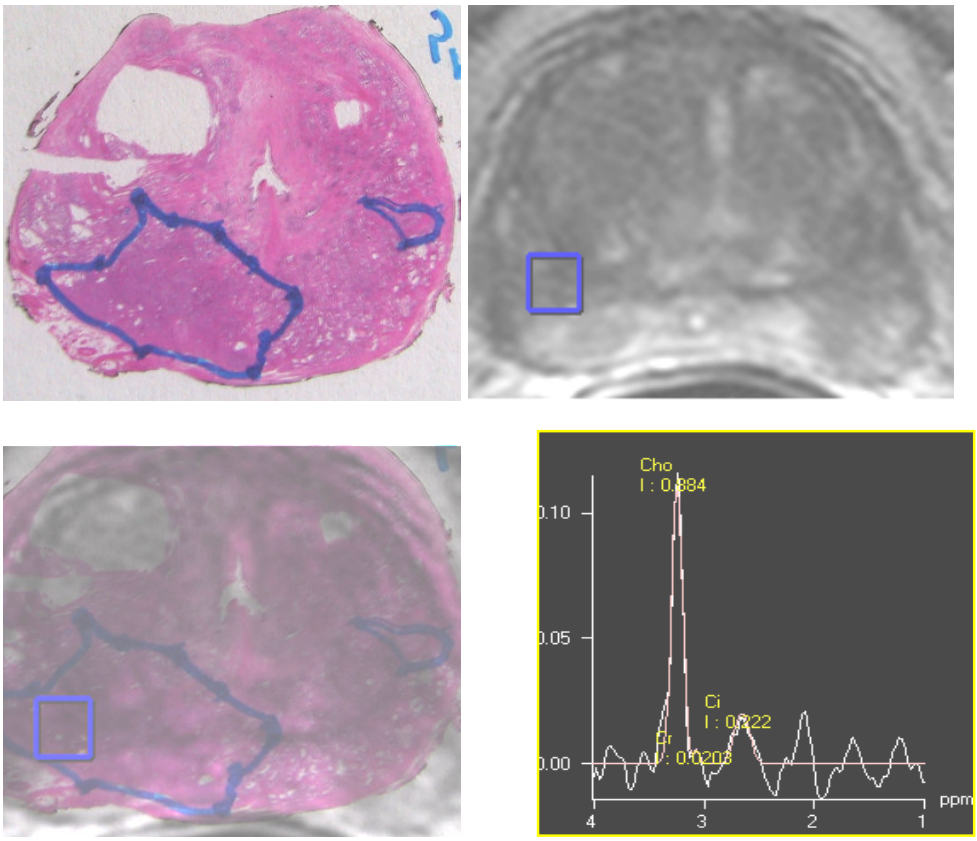

Fig.15. Fusion imaging of histology, MRI and MRS and related neoplastic spectrum.

We classified the obtained spectra as normal if (Cho+Cr)/Cit ratio was <2 SD, uncertain if ratio was <2-3SD> and pathologic if ratio was >3

SD from the normal. On this basis we find a cut-off value (0.47) that may be used to discriminate between normal tissue (<2 SD or <2-3 SD>) and cancer (>3 SD) in peripheral zone (table 3).

The ROC curve confirmed our cut-off as a very good one (sensitivity 100%, specificity 89.4 (figure 16).

	(Cho+Cr)/Cit
Normal	< 0.47
Cancer	> 0.47

Table 3: The cut-off value for (Cho+Cr)/Cit ratio.

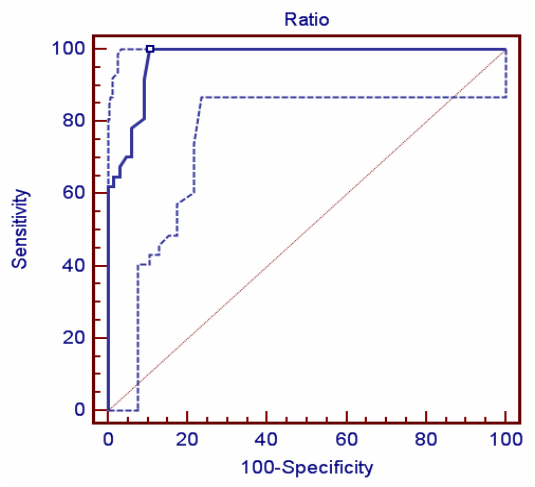

Figure 16. Sensitivity and specificity of ROC curves

Furthermore we classified patients of our study basing on Gleason score resulting from histologic analysis. We obtained five degree of Gleason score (3+3, 3+4, 4+3, 3+5 and 4+5). For each group we plotted the different values of Cho+Cr)/Cit ratio and we demostrated (fig.17) a significative correlation between (Cho+Cr)/Cit ratio and Gleason score ($r=0.5816$, $p<0.0001$).

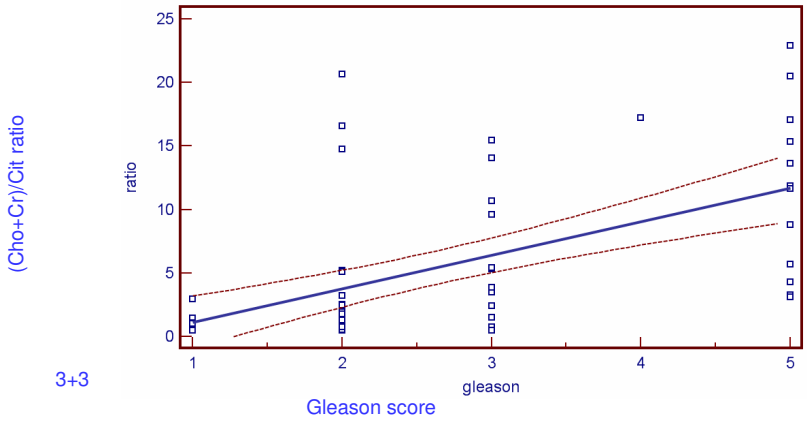

Figure 17. Correlation between (Cho+Cr)/Cit ratio and Gleason score.

DISCUSSION

MR imaging keep on evolving in the diagnostic evaluation of prostate cancer. It has found a role as a local staging modality for differentiation between patients with organ-confined cancer and those with extracapsular tumor extension [56]. New treatment strategies (eg. imaging-guided brachytherapy [57], laser therapy [58], and cryotherapy [59]) and the concept of watchful waiting [60] require an extension of diagnostic imaging beyond staging to providing more precise information about tumor presence and location. Accurate tumor localization will allow greater intensity of treatment to areas of the prostate gland where cancer is present, which will ideally increase the effectiveness of treatment while reducing treatment-related morbidity. In addition, information about tumor growth with accurate tumor localization and sizing may also assist selection and maintenance of a watchful waiting strategy that may obviate repeated biopsies. Knowledge of tumor location may also be of use in patients with elevated prostate-specific antigen level but repeatedly negative findings at prostatic biopsy. In that clinical setting, knowledge of tumor location may help guide future biopsies.

Current diagnostic strategies have limitations in tumor detection and localization. Transrectal US fails to depict as many as 8%–30% of

lesions palpable at digital rectal examination. Transrectal US also has a high false-positive rate in cancer evaluation because only 20% of hypoechoic lesions (US finding most indicative of cancer) are malignant [61]. MR imaging with a combined endorectal and phased-array coil has demonstrated a high sensitivity (91%) but low specificity (27%) in tumor lateralization [5]. Initial reports about 3D MR spectroscopic imaging show that the ability of this technique to distinguish between cancer, benign prostatic hypertrophy, and normal prostatic tissue suggests that the addition of MRS to clinical MRI may increase the specificity of MR imaging in tumor detection and localization [62].

In our study, we evaluated this hypothesis by correlating results with MRI, MRS alone, or both to those with step-section histopathologic examination in patients who underwent prostatectomy.

Data points on the histogram indicated a significantly better performance with combined MRI and MRS than with MRI alone. MRI+MRS demonstrated a better sensitivity and accuracy in tumor localization respect to MRI alone. The accuracy we obtained using combined MRI and MRS for tumor lateralization (right or left prostatic lobe) was 88%, as indicated on literature [47]. A negative result with combined MRI and MRS excluded the presence of cancer

with high probability (negative predictive value, 64% VS 53% of MRI alone) (Fig.15).

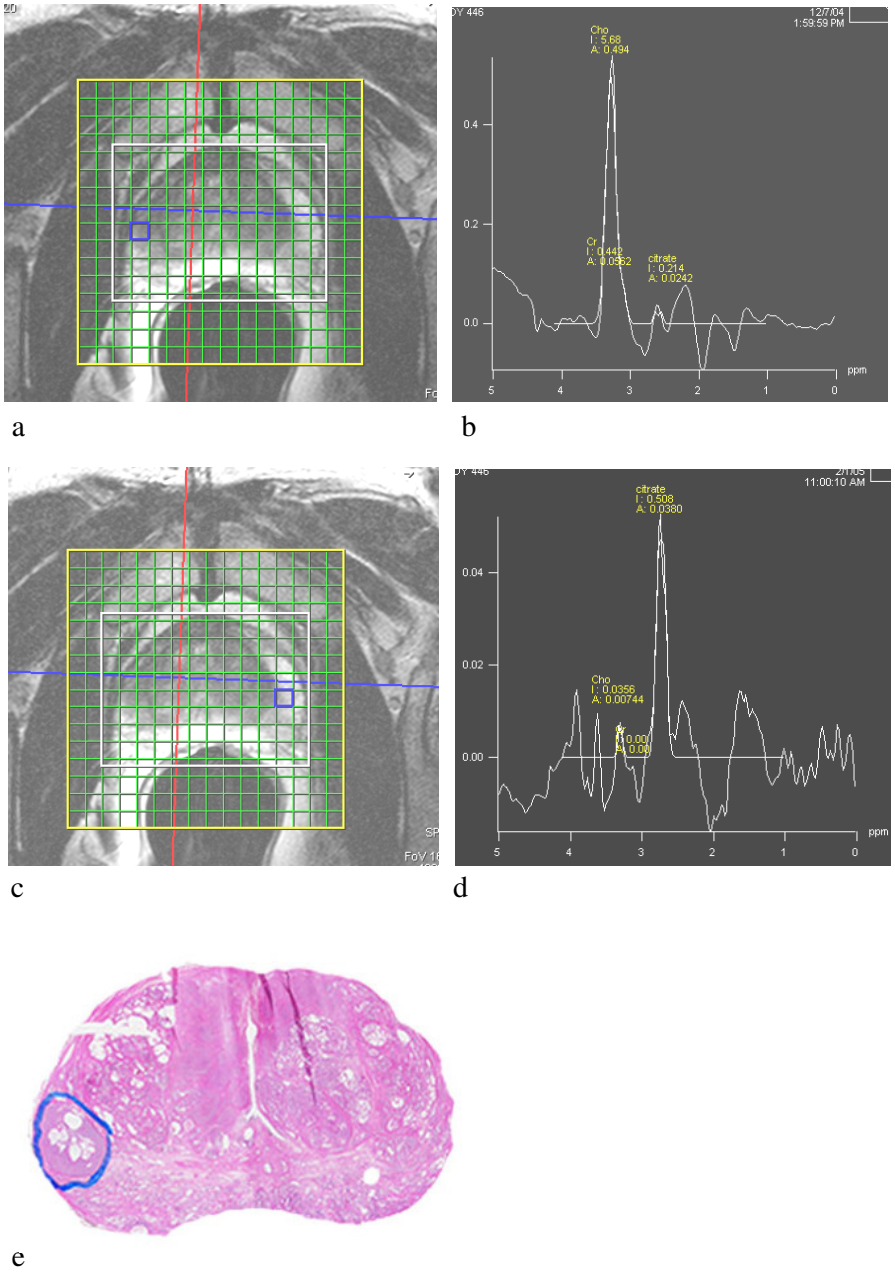

Fig.15 Axial T2- weighted images from an FSE sequence of a 61-year-old patient with a PSA level of 8.7 ng/ml and a histologically proven prostate carcinoma of the right side (e) with demonstration of a tumour voxel (a,b) and a control benigne voxel from the opposite side (c,d).

Our study showed also that we can use the cut-off value of (Cho+Cr)/Cit ratio of 0.47 to discriminate between cancer and normal prostatic tissue in the peripheral zone (sensitivity 89.2%; specificity 91%, p=0.0001).

Preliminary findings suggest that small, low-grade tumors may be undetected with MRS because the severity of metabolite alteration correlates with tumor aggressiveness. High-grade cancers (Gleason scores 7 and 8) revealed highly elevated choline resonances, whereas lower grade tumors (Gleason scores 4 and 5) showed slightly elevated choline levels only [63].

However our study had some limitations, including a small number of patients. Two radiologists compared the tumor locations with the histopathologic data after having read MR an MRS images, and this may have introduced information bias.

Furthermore our experience with MRS increased during the study and thereby resulted in improved quality of the spectra and reduced examination time; however these factors were not evaluated in detail. MRI was performed after prostate biopsy, with at least 4 weeks between the two procedures. This factor may have introduced spectral degradation [64].

Moreover it is important to stress the fact that traditionally sextant biopsy has been regarded as the standard of reference for nonsurgical cancer localization [65]. In our experience we have noticed that the reality is not always this one. In fact sextant biopsy has some important limitations which cannot be forgotten, for example its completely dependency by the operator but most important its limited sensitivity due to sampling error expecially in the prostate apex. In particular, this last result is probably associated with under sampling the apex during transrectal ultrasound guided biopsy since the prostate apex is smaller and less easily visualized, and at biopsy the sample is obtained from the tissue superior to the needle tip [66,67].

On the other hand, these increasingly recognized limitations of sextant biopsy has provoked interest in endorectal MRI and MRS as alternative methods of tumor evaluation, expecially when MRI and MRS are performed in a combined way [68].

Logically we are not suggesting that MRI plus MRS should replace sextant biopsies for tumour diagnosis, but we have noticed that all the methodological problems intrinsic to the sampling technique is putting sextant biopsies in an unfair light in regard to MRI with MRS.

We believe the clinical implications of improved prostate cancer localization with MRS apply (a) for patients with increasing prostate-

specific antigen levels and negative US-guided biopsy (for souspicious lesions) results; (b) for evaluation of tumor location and of the distance to the neurovascular bundle and the prostate capsule to determine if nerve-sparing surgery is possible; and (c) for planning of intensity-modulated radiation therapy [69] , which requires exact localization of the prostate cancer to administer an extra boost of radiation in addition to the normal dose.

In conclusion, findings in this study demonstrate the potential usefulness of combined morphologic and metabolic information about prostate cancer in clinical practice and provide an analysis of this new method. Our findings showed that the addition of MRS to MRI provides better detection and localization of prostate cancer, with sensitivity, accuracy and NPV higher than those with MR imaging alone. This suggest that if this technique is included in the MR imaging protocol, the localization of prostate cancer in patients will improve.

REFERENCES

1. Hricak H, White S, Vigneron D et al: Carcinoma of the prostate gland: MR imaging with pelvic phased-array coils versus integrated endorectal-pelvic phased-array coils. Radiology 1994; 193:703–705

2. Huch Boni RA, Meyenberger C, Pok Lundquist J et al: Value of endorectal coil versus body coil MRI for diagnosis of recurrent pelvic malignancies. Abdom Imaging 1996; 21:345–352

3. Salo JO, Kivisaari L, Rannikko S et al: Computerized tomography and transrectal ultrasound in the assessment of local extension of prostatic carcinoma before radical retropubic prostatectomy. J Urol 1987; 137:435–438

4. Ellis JH, Tempany C, Sarin MS et al: MR imaging and sonography of early prostatic cancer: pathologic and imaging features that influence identification and diagnosis. AJR 1994; 162:865–872

5. Engeler CE, Wasserman NF, Zhang G: Preoperative assessment of prostatic carcinoma by computerized tomography. Weaknesses and new perpectives. Urology 1992; 490:346–349

6. McNeal JE: Normal and pathological anatomy of the prostate. Urology 1981;17:11–16

7. Coakley FV, Hricak H: Radiologic anatomy of the prostate gland: a clinical approach. Radiol Clin North Am 2000; 38:15–30

8. Salo JO, Kivisaari L, Rannikko S et al: Computerized tomography and transrectal ultrasound in the assessment of local extension of prostatic carcinoma before radical retropubic prostatectomy. J Urol 1987; 137:435–438

9. Ellis JH, Tempany C, Sarin MS et al: MR imaging and sonography of early prostatic cancer: pathologic and imaging features that influence identification and diagnosis. AJR 1994; 162:865–872

10. Engeler CE, Wasserman NF, Zhang G: Preoperative assessment of prostatic carcinoma by computerized tomography. Weaknesses and new perpectives. Urology 1992; 490:346–349

11. Barentsz JO, Engelbrecht MR, Witjes JA et al: MR imaging of the male pelvis. Eur Radiol 1999; 9(9):1722-36. Review

12. Bartolozzi C, Crocetti L, Menchi I et al: Endorectal magnetic resonance imaging in local staging of prostate carcinoma. Abdom Imaging 2001; 26:111–122

13. Rorvik J, Haukass S: Magnetic resonance imaging of the prostate. Curr Opin Urol. 2001 Mar; 11(2):181-8. Review

14. Getty DJ, Seltzer SE, Tempany CMC et al: Prostate cancer: relative effects of demographic, clinical, histologic, and MR imaging variables on the accuracy of staging. Radiology 1997; 204:471–479

15. Lane RB, Lane CG, Mangold KA, Johnson MH et al:Needle biopsies of the prostate: what constitutes adequate histologic sampling? Arch Pathol Lab Med 1998 Sep; 122(9):833-5

16. Steinberg DM, Sauvageot J, Piantadosi S et al: Correlation of prostate needle biopsy and radical prostatectomy Gleason grade in academic and community settings. Am J Surg Pathol 1997 May; 21(5):566-76

17. D'Amico AV, Whittington R, Malkowicz SB et al: Combination of the preoperative PSA level, biopsy Gleason score, percentage of positive biopsies, and MRI T-stage to predict early PSA failure in men with clinically localized prostate cancer. Urology 2000; 55:572–577

18. Haggman MJ, Macoska JA, Wojno KJ et al: The relationship between prostatic intraepithelial neoplasia and prostate cancer: critical issues. J Urol 1997 Jul; 158(1):12-22. Review

19. Reyes AO, Swanson PE, Carbone JM et al: Unusual histologic types of high-grade prostatic intraepithelial neoplasia. Am J Surg Pathol 1997 Oct; 21(10):1215-22

20. Presti JC Jr: Prostate cancer: assessment of risk using digital rectal examination, tumor grade, prostate-specific antigen, and systematic biopsy. Radiol Clin North Am 2000; 38:49–58

21. Slawin KM, Ohori M, Dillioglugil O et al: Screening for prostate cancer: an analysis of the early experience. CA Cancer J Clin 1995; 45:134–138

22. Huncharek M, Muscat J: Serum prostate specific antigen as a predictor of staging abdominal/pelvic CT in newly diagnosed prostate cancer. Abdom Imaging 1996; 21:364–367

23. Morote J, Encabo G, Lopez M et al: Prediction of prostate volume based on total and free serum prostate-specific antigen: is it reliable? Eur Urol 2000; 38:91–95

24. Rossigno M, Scattoni V, Bestini R et al: Diagnosis of prostate cancer. State of the art. Minerva Urol Nefrol. 2004 Jun; 56(2):123-45. Review

25. White S, Hricak H, Forstner R et al: Prostate cancer: effect of postbiopsy hemorrhage on interpretation of MR images. Radiology 1995;195:385–390

26. Huch Boni RA, Boner JA, Lutolf UM et al: Contrast-enhanced endorectal coil MRI in local staging of prostate carcinoma. J Comput Assist Tomogr 1995; 19:232–237

27. Mirowitz SA, Brown JJ, Heiken JP: Evaluation of the prostate and prostatic carcinoma with gadolinium-enhanced endorectal coil MR imaging. Radiology 1993; 186:153–156

28. Montie JE: Staging of prostate cancer. Current TNM classification and future prospects for prognostic factors. Cancer 1995; 75:1814–1818

29. Ikonen S, Karkkainen P, Kivisaari L et al: Magnetic resonance imaging of clinically localized prostatic cancer. J Urol 1998; 159:915–919

30. Jager GJ, Barentz JO, Ruijter ETG et al: Primary staging of prostate cancer. Eur Radiol 1996; 6.134–139

31. Jager GJ, Rujter ETG, van de Kaa CA et al : Local staging of prostate cancer with endorectal MR imaging: correlation with histopathology. AJR 1996; 166:845–852

32. Fournier G, Valeri A, Mangin P et al: Prostate cancer: Diagnosis and staging. Ann Urol (Paris). 2004 Oct; 38(5):207-24. Rewiew

33. Huch Boni RA, Boner JA, Debatin JF et al: Optimization of prostate carcinoma staging: comparison of imaging and clinical methods. Clin Radiol 1995; 50:593–596

34. Lencioni R, Menchi I, Paolicchi A et al: Prediction of pathological tumor volume in clinically localized prostate cancer: value of endorectal coil magnetic resonance imaging. MAGMA 1997; 5:117–12

35. Tsuda K, Yu KK, Coakley FV et al: Detection of extracapsular extension of prostate cancer: role of fat suppression endorectal MRI. J Comput Assist Tomogr 1999; 23:74–78

36. White S, Hricak H, Forstner R et al: Prostate cancer: effect of postbiopsy hemorrhage on interpretation of MR images. Radiology 1995;195:385–390

37. Adusumilli S, Pretorius ES: Magnetic resonance imaging of prostate cancer. Semin Urol Oncol. 2002 Aug; 20(3):192-210

38. Engelbrecht MR, Jager GJ, Laheij RJ et al: Local staging of prostate cancer using magnetic resonance imaging: a meta analysis. Eur Radiol 2002; 12:2294-2302

39. Heuck A, Scheidler J, Sommer B et al: MR imaging of prostate cancer. Radiologe 2003 Jun; 43(6):464-73. Review

40. Jager GJ, Severens JL, Thornbury JR et al: Prostate cancer staging: should MR imaging be used?—a decision analytic approach. Radiology 2000; 215:445–451

41. Rorvik J, Halvorsen OJ, Allbrektsen G et al: MRI with an endorectal coil for staging of clinically localised prostate cancer prior to radical prostatectomy. Eur Radiol 1999; 9:29–34

42. Yu KK, Hricak H: Imaging prostate cancer. Radiol Clin North Am 2000; 38:59–85

43. Coakley FV, Kurhanewicz J, Lu Y et al: Prostate cancer tumor volume: measurements with endorectal MR and MR spectroscopic imaging. Radiology 2002; 223:91-97

44. Kurhanewicz J, Swanson MG, Nelson SJ et al: Combined magnetic resonance imaging and spectroscopic imaging approach to molecular imaging of prostate cancer. J Magn Reson Imaging 2002; 16(4):451-63

45. Mueller-Lisse UG, Scherr M: 1H magnetic resonance spectroscopy of the prostate. Radiologe. 2003 Jun; 43(6):481-8. Review

46. Rajesh A, Coakley FV: MR imaging and MR spectroscopic imaging of prostate cancer. Magn Reson Imaging Clin N Am. 2004 Aug; 12(3):557-79. Review

47. Scheidler J, Hricak H, Vigneron DB et al: Prostate cancer: localization with three-dimensional proton MR spectroscopic imaging-clinicopathologic study. Radiology 1999; 213(2):473-480

48. Quinn M, Babb P: Patterns and trends in prostate cancer incidence, survival prevalence and mortality. Part I. International comparisons. Br J Urol Int 2002; 90:162-173

49. Levi F, Lucchini F, Negri E, et al: Leveling of prostate cancer mortality in Western Europe. Prostate 2004; 60:46-52

50. Sanchez-Chapado M, Angulo JC, Ibarburen C, et al: Comparison of digital rectal examination, transrectal ultrasonography, and multicoil magnetic resonance imaging for preoperative evaluation of prostate cancer. Eur Urol 1997; 32:140-149

51. Ito H, Kamoi K, Yokoyama K, Yamada K, Nishimura T: Visualization of prostate cancer using dynamic contrast-enhanced MRI: comparison with transrectal power Doppler ultrasound. Br J Radiol 2003; 76:617–624

52. Kurhanewicz J, Vigneron DB, Hricak H et al: Three-dimensional H-1 MR spectroscopic imaging of the in situ human prostate with high (0.24–0.7-cm^3) spatial resolution. Radiology 1996; 198:795-805

53. Kurhanewicz J, Swanson MG, Nelson SJ, Vigneron DB: Combined magnetic resonance imaging and spectroscopic imaging approach to molecular imaging of prostate cancer. (review) J Magn Reson Imaging 2002; 16:451 -463

54. Scheenen TWJ, Klomp DWJ, Röll SA et al: Fast acquisition-weighted three dimensional proton MR spectroscopic imaging of the human prostate. Magn Reson Med 2004; 52:80–88

55. Landis JC, Koch GC: The measurement of observer agreement for categorical data. Biometrics 1977; 33:159-174

56. Yu KK, Hricak H, Alagappan R et al: Detection of extracapsular extension of prostate carcinoma with endorectal and phased-array coil MR imaging: multivariate feature analysis. Radiology 1997; 202:697-702

57. Stokes SH, Real JD, Adams PW et al: Transperineal ultrasound-guided radioactive seed implantation for organ-confined carcinoma of the prostate. Int J Radiat Oncol Biol Phys 1997; 37:337-341

58. Amin Z, Lees WR, Bown SG. Technical note: interstitial laser photocoagulation for the treatment of prostatic cancer. Br J Radiol 1993; 66:1044-1047

59. Lee F, Bahn DK, McHugh TA et al: US-guided percutaneous cryoablation of prostate cancer. Radiology 1994; 192:769-776

60. Chodak GW, Thisted RA, Gerber GS et al. Results of conservative management of clinically localized prostate cancer. N Engl J Med 1994; 330:242-248

61. Lee F, Torp-Pedersen S, Littrup PJ et al: Hypoechoic lesions of the prostate: clinical relevance of tumor size, digital rectal examination, and prostate-specific antigen. Radiology 1989; 170:29-32

62. Kurhanewicz J, Vigneron DB, Hricak H et al: Three-dimensional H-1 MR spectroscopic imaging of the in situ human prostate with high (0.24–0.7-cm^3) spatial resolution. Radiology 1996; 198:795-805

63. Vigneron DB, Males R, Noworolski S et al: 3D MRSI of prostate cancer: correlation with histologic grade (abstr) In: Proceedings of the Sixth Meeting of the International Society for Magnetic Resonance in Medicine. Berkeley, Calif: International Society for Magnetic Resonance in Medicine, 1998; 487

64. Quayyum A, Coakley FV, Lu Y, et al: Organconfined prostate cancer: effect of prior transrectal biopsy on endorectal MRI and MR spectroscopic imaging. AJR Am J Roentgenol 2004; 183:1079-1083

65. Horndalsveen Berild G, Nielsen K: Accuracy in core biopsy of the prostate. An autopsy study. Urol Int 1986; 41: 276

66. Öbek C, Louis P, Civantos F et al: Comparison of digital rectal examination and biopsy results with the radical prostatectomy specimen. J Urol 1999; 161: 494

67. Salomon L, Colombel M, Patard J J et al: Value of ultrasound-guided systematic sextant biopsies in prostate tumor mapping. Eur Urol 1999; 35: 289

68. Yu K K, Hricak H, Alagappan R et al: Detection of extracapsular extension of prostate carcinoma with endorectal and phased-array coil MR imaging multivariate feature analysis. Radiology 1997; 202: 697

69. Zelefsky MJ, Fuks Z, Leibel SA. Intensity-modulated radiation therapy for prostate cancer. Semin Radiat Oncol 2002; 12:229-237